

Statistical distribution of current helicity in solar active regions over the magnetic cycle.

Y. Gao^{1*}, T. Sakurai^{2†}, H. Zhang^{1‡}, K.M. Kuzanyan^{1,2,3§}, D. Sokoloff^{1,4¶}

¹*Key Laboratory of Solar Activity, National Astronomical Observatories, Chinese Academy of Sciences, Beijing 100012, China*

²*National Astronomical Observatory of Japan, 2-21-1 Osawa, Mitaka, Tokyo 181-8588*

³*IZMIRAN, Troitsk, Moscow Region 142190, Russia*

⁴*Department of Physics, Moscow State University, Moscow, 119992, Russia*

20120926

ABSTRACT

The current helicity in solar active regions derived from vector magnetograph observations for more than 20 years indicates the so-called hemispheric sign rule; the helicity is predominantly negative in the northern hemisphere and positive in the southern hemisphere. In this paper we revisit this property and compare the statistical distribution of current helicity with Gaussian distribution using the method of normal probability paper. The data sample comprises 6630 independent magnetograms obtained at Huairou Solar Observing Station, China, over 1988-2005 which correspond to 983 solar active regions. We found the following. (1) For the most of cases in time-hemisphere domains the distribution of helicity is close to Gaussian. (2) At some domains (some years and hemispheres) we can clearly observe significant departure of the distribution from a single Gaussian, in the form of two- or multi-component distribution. (3) For the most non-single-Gaussian parts of the dataset we see co-existence of two or more components, one of which (often predominant) has a mean value very close to zero, which does not contribute much to the hemispheric sign rule. The other component has relatively large value of helicity that often determines agreement or disagreement with the hemispheric sign rule in accord with the global structure of helicity reported by Zhang et al. (2010).

Key words: Sun: magnetic fields – Sun: activity – Sun: interior

1 INTRODUCTION

Recently there has been significant progress in collection and interpretation of observational data on vector magnetic fields in solar active regions which enables us to compute the values of current helicity (a measure of departure of magnetic fields from mirror symmetry) averaged over active regions (Seehafer 1990; Pevtsov, Canfield and Metcalf 1995; Bao and Zhang 1998). The data have been averaged over latitude and time in the solar cycle as well (Zhang et al. 2010). The research so far has demonstrated important properties of this quantity and its regular variation in the course of the solar cycle. The helicity is generally negative in the northern hemisphere and positive in the southern hemisphere; the so-called hemispheric sign rule (HSR) for helicity. This rule, however, may occasionally be violated in the activity minimum periods (Hagino and Sakurai 2005; Zhang et al. 2010; Hao and Zhang 2012).

Helicity in the solar atmosphere has been noted as an important agent which constrains magnetic field dissipation in the solar corona. Current helicity plays an important role in the solar dynamo theory as an observational proxy of the α -effect as it controls a dynamical back-reaction of the magnetic field to the motion of the media which suppresses and stabilizes the generation of the magnetic field (e.g. Kleeorin et al. 2003; Zhang et al. 2006). From a theoretical point of view the average helicity has the meaning of a quantity averaged over an ensemble of turbulent fluctuations in a small physical volume. This physical volume may contain a limited number of convective cells, and so we may expect it to vary significantly in space and time. The data on current helicity are indeed very fluctuating within a given active region as well as during its evolution (Zhang et al. 2002). Similar fluctuations can be observed in the current helicity averaged over latitude and time in the solar cycle.

However, the observation of current helicity is a complex process which deals with initially imperfect data and involves highly non-trivial reduction processes. These difficulties must be overcome by collecting reliable datasets, because noise in the data will degrade the reliability in the analysis (e.g. Abramenko et al. 1996; Bao and Zhang 1998; Bao et al. 2001; Hagino and Sakurai 2004, 2005). For better understanding of the reliability of the analysis of current helicity previously undertaken, we hereby aim to study its statistical distribution.

* Email: gy@bao.ac.cn

† Email: sakurai@solar.mtk.nao.ac.jp

‡ Email: hzhang@bao.ac.cn

§ Email: kuzanyan@gmail.com

¶ Email: sokoloff.dd@gmail.com

On the other hand the current helicity as a quantity responsible for mirror asymmetry of solar magnetic field is expected to be fluctuating also from a theoretical viewpoint: A usual expectation is that the degree of mirror asymmetry in dynamo mechanisms will be about 10%. This practical estimate as originating from Parker (1955) means that we have to isolate stable features of current helicity distributions on a background of physical fluctuation which may be ten times greater than the average value. This fluctuation is not due to observational uncertainties and cannot be reduced by improvement of observational techniques.

The expected substantial fluctuation in the current helicity data has to be carefully taken into account in estimating the averaged values of current helicity. Intrinsic (physical and true) dispersion in the current helicity data around its mean value is, however, interesting by itself.

The probability distribution of current helicity may be substantially non-Gaussian. The point is that physical processes responsible for the fluctuating nature of solar plasma can be considered as an action of a product of independent evolutionary operators rather than a sum of them resulting usually in a Gaussian distribution. On the other hand, averaging over an active region smoothes fluctuation and supports the Gaussian nature of distribution.

Because of this, the statistical properties of current helicity deserve to be addressed in full detail. Previously, the statistical distribution of current helicity has been addressed only briefly as a part of more general studies (e.g. Sokoloff et al. 2008).

In this paper we consider the distribution of available data over the hemispheres of the Sun and their changes over solar cycles. We compare this distribution with a Gaussian and separate the part of the data which significantly deviates from a single Gaussian distribution. Then, we consider the spatial and temporal properties of this part in comparison with the other (Gaussian) part of the data. We shall see that both parts exhibit similar properties and behavior over the solar cycle.

2 OBSERVATIONAL DATA SET

This study is based on the data of photospheric vector magnetograms of solar active regions obtained at Huairou Solar Observing Station, China. The same database systematically covering 18 consecutive years (1988-2005) was used in Zhang et al. (2010). The parameters adopted there are α_{av} (the average **value** of $\alpha; \nabla \times \mathbf{B} = \alpha \mathbf{B}$) and H_c (the integrated current helicity; $H_c = \Sigma J_z B_z$). In the present analysis we will use the same parameters. (the inte-

grated current helicity; $H_c = \sigma J_z B_z$) First, we analyze the entire database that comprises 6630 magnetograms of 983 different active regions (in terms of NOAA region numbers). We are going to build our statistical analysis for the whole bulk of available data. The majority of active regions are represented by only one or very few magnetograms. However, there are a few active regions that were recorded in 20 or more magnetograms. In the next step we select one magnetogram for an active region. Sometimes, and for some active regions that were observed within a short time interval, the helicity parameters may be close with each other. For these magnetograms, we select the one located nearest to the center of the solar disk. Furthermore, we try to avoid choosing the magnetograms of rapidly emerging active regions, except for those regions which were recorded in only one magnetogram. Nonetheless, this occurs rather rarely because such active regions are usually large and well observed over several days.

3 METHOD OF STATISTICAL ANALYSIS

We address the probability distribution of current helicity and its deviation from Gaussian as it follows from observational data by two statistical tools.

First of all, we divide the data into two hemispheres and produce histograms of the current helicity distribution for certain time intervals which contain 50 measurements. We then approximate them by multiple Gaussians. In practice it appears that a mixture of two Gaussians is sufficient to reproduce the histograms with a reasonable accuracy.

This method, being very practical, may miss in principle substantial deviations from Gaussian statistics which occurs with low probability, i.e. intermittent features in the probability distribution. A tool to address an intermittent feature is the so-called Normal Probability Paper (NPP) test which is organized as follows (see, e.g., Chernoff and Lieberman 1954).

Let our set contain N active regions. Let n active regions have current helicity density χ_c lower than x . Then the probability for χ_c to be lower than x is estimated as $P = n/N$. Let ξ be a Gaussian variable with the same mean value μ and standard deviation σ as χ_c and let y be the value for which the probability for $(\xi - \mu)/\sigma$ to be lower than y is P . The results for various x values are plotted in the (x, y) -plane and can be compared with the cumulative distribution function (CDF) for a Gaussian distribution which gives a straight line in this coordinate space. If the observational data deviate substantially from this straight line, it

is an indication of a non-Gaussian nature of observational data (see e.g. Sokoloff et al. 2008 for details).

For illustration let us produce a set of random Gaussian variable xx_1 ($N = 1500$, $\mu_1 = 0.098$, and $\sigma_1 = 1.05$) by IDL function “randomn”. Then we produce another set of random Gaussian variable xx_2 ($\mu_2 = -0.28$ and $\sigma_2 = 0.42$). The GAUSS_CVF function computes the cutoff value V in a standard Gaussian distribution with a mean of 0.0 and a variance of 1.0 such that the probability that a random variable X is greater than V is equal to a user-supplied probability P (see Figure 1). The upper panel shows the probability distribution functions (PDFs) of two Gaussian components and their sum (with equal weights). In the bottom panel we show the relationship between the variable and the Gaussian CDF with the same mean value and standard deviation for three kinds of variables. The correlation for Gaussian variables is well fit by a straight line but not for the sum of the components, as shown in Figure 1 by the red curve. The slope of the straight line is determined by the mean value, and the y -intercept is determined by the standard deviation of the corresponding dataset.

4 RESULTS

The entire sample includes 983 active regions, in which 464 (519) in the northern (southern) hemisphere, respectively. Tables 1–4 present the detailed information about the Gaussian fitting to the distribution function of the observed parameters. The columns indicate; “#”: the sequence number of subgroups, “Start” (“End”): the earliest (last) measurement in the subgroup, δT : the length of the time epoch between “Start” and “End”, μ_0 and σ_0 : the mean value and standard deviation of the subgroup, and μ_1 , σ_1 , A_1 , μ_2 , σ_2 and A_2 are the parameters defining the components of the sum of Gaussian function in the form:

$$f(x) = \frac{A_1}{\sqrt{2\pi}\sigma_1} \exp\left[-\frac{(x - \mu_1)^2}{2\sigma_1^2}\right] + \frac{A_2}{\sqrt{2\pi}\sigma_2} \exp\left[-\frac{(x - \mu_2)^2}{2\sigma_2^2}\right], \quad (1)$$

where the component with subscript “1” represents the component with a greater amplitude; $A_1 \geq A_2$. The fitting is not made on the PDF but is made for CDF; the function we use for the fitting is actually the integral of Equation (1), namely the sum of two error functions. The “Error” denotes the deviation of the observed values from the fitting with the sum of two error functions. The “No” column records the number of data points in each subgroup.

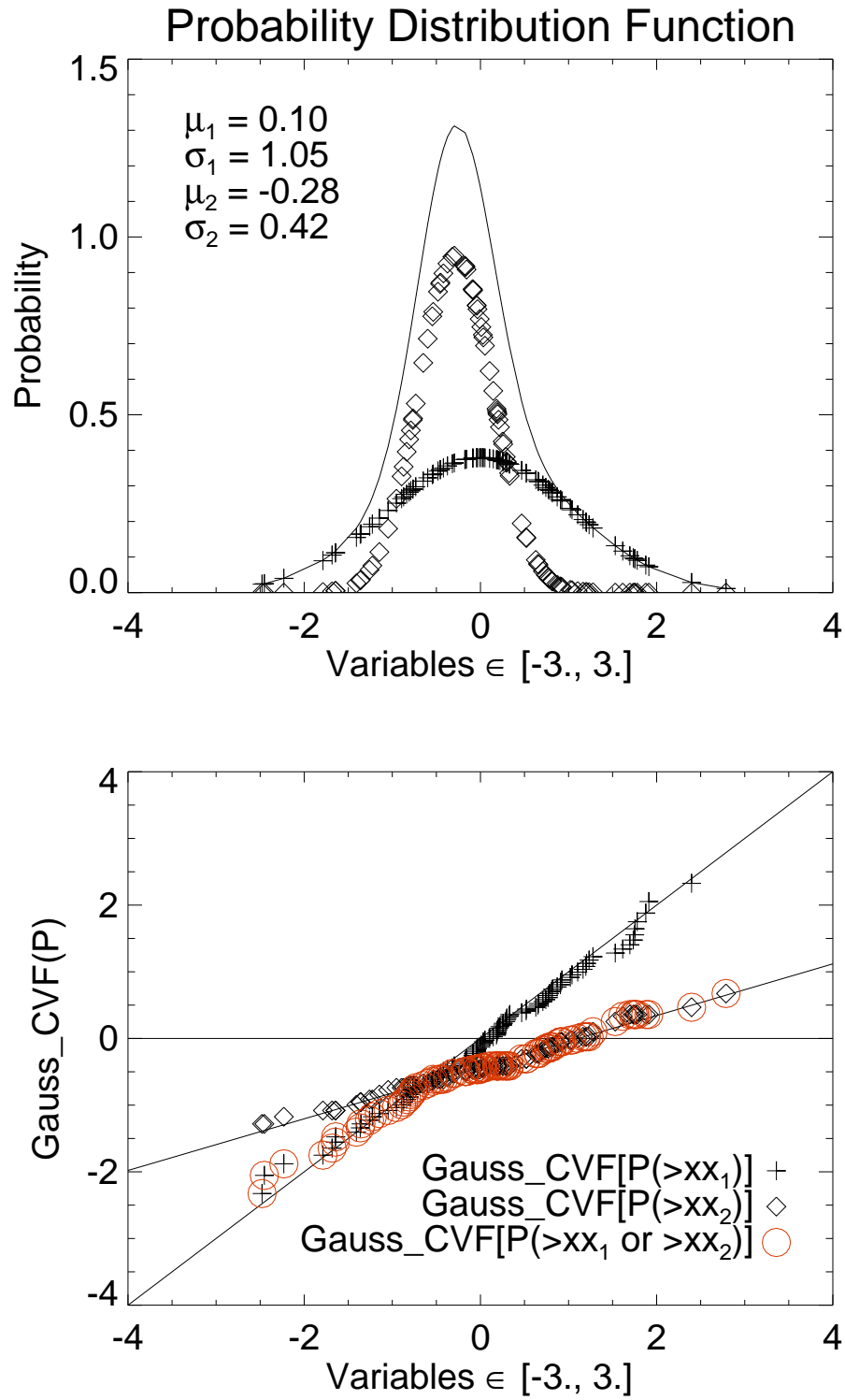


Figure 1. Probability Distribution Function (PDF) of a set of random Gaussian variable (upper panel) and correlation between the variable and the Gaussian Cumulative Distribution Function (CDF) with the same mean value and standard deviation (bottom panel).

Table 1. Results of fitting to the data of α_{av} for ten data subgroups in the northern hemisphere. The fit error is standard deviation of the fitting curve from the observed values. The values of amplitudes A_1 and A_2 for cases when the second component is significant ($A_2 > A_1/2$) are underlined.

#	Start	End	δT	μ_0	σ_0	μ_1	σ_1	A_1	μ_2	σ_2	A_2	Error	No
1	Apr-16,1988	May-11,1990	755	-0.0088	0.0176	-0.0046	0.0154	0.8932	-0.0405	0.0061	0.1068	0.0948	50
2	May-20,1990	Jan-22,1992	612	-0.0119	0.0231	-0.0057	0.0160	<u>0.6506</u>	-0.0226	0.0347	<u>0.3494</u>	0.1356	50
3	Jan-25,1992	Dec-18,1993	693	0.0021	0.0227	-0.0031	0.0071	<u>0.5360</u>	0.0094	0.0353	<u>0.4640</u>	0.1364	50
4	Dec-26,1993	May-24,1998	1610	-0.0065	0.0169	-0.0044	0.0231	<u>0.5651</u>	-0.0082	0.0088	<u>0.4349</u>	0.1840	50
5	May-31,1998	Jul-22,1999	417	-0.0042	0.0161	-0.0034	0.0126	0.9609	-0.0843	0.0055	0.0391	0.1330	50
6	Jul-23,1999	Jun-11,2000	324	-0.0030	0.0128	-0.0026	0.0176	<u>0.5978</u>	-0.0029	0.0058	<u>0.4022</u>	0.1127	50
7	Jun-12,2000	Dec-21,2000	192	-0.0046	0.0140	-0.0016	0.0091	0.8807	-0.0402	0.0287	0.1193	0.1369	50
8	Dec-25,2000	Sep-02,2001	251	0.0005	0.0200	0.0035	0.0306	<u>0.5017</u>	-0.0015	0.0071	<u>0.4983</u>	0.1204	50
9	Sep-22,2001	Jun-28,2003	644	-0.0038	0.0177	-0.0045	0.0168	0.9779	0.2665	0.3073	0.0221	0.1293	50
10	Jul-5,2003	Dec-23,2005	902	-0.0028	0.0123	-0.0057	0.0211	<u>0.5652</u>	0.0008	0.0035	<u>0.4348</u>	0.2200	14

Table 2. Results of fitting to the data of α_{av} for eleven data subgroups in the southern hemisphere. The fit error is standard deviation of the fitting curve from the observed values. The values of amplitudes A_1 and A_2 for cases when the second component is significant ($A_2 > A_1/2$) are underlined.

#	Start	End	δT	μ_0	σ_0	μ_1	σ_1	A_1	μ_2	σ_2	A_2	Error	No
1	Apr-26,1988	Feb-25,1990	670	-0.0039	0.0235	-0.0003	0.0181	0.8223	-0.0227	0.0487	0.1777	0.0993	50
2	Mar-08,1990	Aug-11,1991	521	0.0068	0.0254	0.0027	0.0162	0.8035	0.0283	0.0542	0.1965	0.1364	50
3	Aug-12,1991	May-08,1992	270	0.0053	0.0165	0.0020	0.0198	0.6668	0.0128	0.0096	0.3332	0.0807	50
4	Jun-16,1992	Jul-21,1993	400	0.0090	0.0206	0.0008	0.0123	0.6766	0.0287	0.0266	0.3234	0.0931	50
5	Jul-29,1993	Aug-27,1996	1125	0.0038	0.0188	-0.0019	0.0106	<u>0.6147</u>	0.0147	0.0279	<u>0.3853</u>	0.0895	50
6	Nov-29,1996	Apr-23,1999	875	0.0053	0.0155	0.0053	0.0208	<u>0.6437</u>	0.0063	0.0057	<u>0.3563</u>	0.1044	50
7	May-19,1999	Apr-12,2000	329	-0.0010	0.0118	-0.0001	0.0091	0.9575	-0.0587	0.0056	0.0425	0.1029	50
8	Apr-15,2000	Nov-20,2000	219	0.0048	0.0160	0.0050	0.0110	0.7850	0.0044	0.0351	0.2150	0.0927	50
9	Nov-27,2000	Oct-11,2001	318	0.0022	0.0231	0.0011	0.0122	<u>0.6237</u>	0.0053	0.0399	<u>0.3763</u>	0.1328	50
10	Oct-22,2001	Oct-27,2003	735	0.0002	0.0170	0.0017	0.0163	0.9807	-0.0694	0.0039	0.0193	0.0992	50
11	Oct-28,2003	Dec-16,2005	780	-0.0045	0.0166	-0.0070	0.0238	<u>0.6532</u>	0.0010	0.0074	<u>0.3468</u>	0.1287	19

Table 1 shows the result of Gaussian fitting/decomposition for α_{av} in the northern hemisphere. We focus on the relation between the sign of mean values of two Gaussian components and the HSR. It is found that there are merely one μ_1 (Row 8) which violates the HSR from Dec-25, 2000 to Sep-02, 2001, while the corresponding μ_2 follows the HSR. In contrast, there are in total three μ_2 's (Rows 3, 9 and 10) which violate the HSR. These epochs are ‘‘Jan-25, 1992’’ to ‘‘Dec-18, 1993’’, ‘‘Sep-22, 2001’’ to ‘‘Jun-28, 2003’’ and ‘‘Jul-5, 2003’’ to ‘‘Dec-23, 2005’’, and their amplitudes A_2 are 0.46, 0.02 and 0.43, respectively. We would like to stress here that the number of data points in the latter subgroup is only 14, which is much less than in the other subgroups. Therefore the fitting for this subgroup is not that reliable. Nevertheless, the fitting in the third subgroup, i.e., from ‘‘Jan-25, 1992’’ to ‘‘Dec-18, 1993’’, is rather convincing. As A_2 is 0.46 for the former group, both components are clearly seen in the second row of Figure 2. In Figure 2 we also give fitting results for the other three epochs. Their distributions are nicely represented by two Gaussians and both components obey the HSR.

Table 2 shows the results of Gaussian fitting/decomposition for α_{av} in the southern

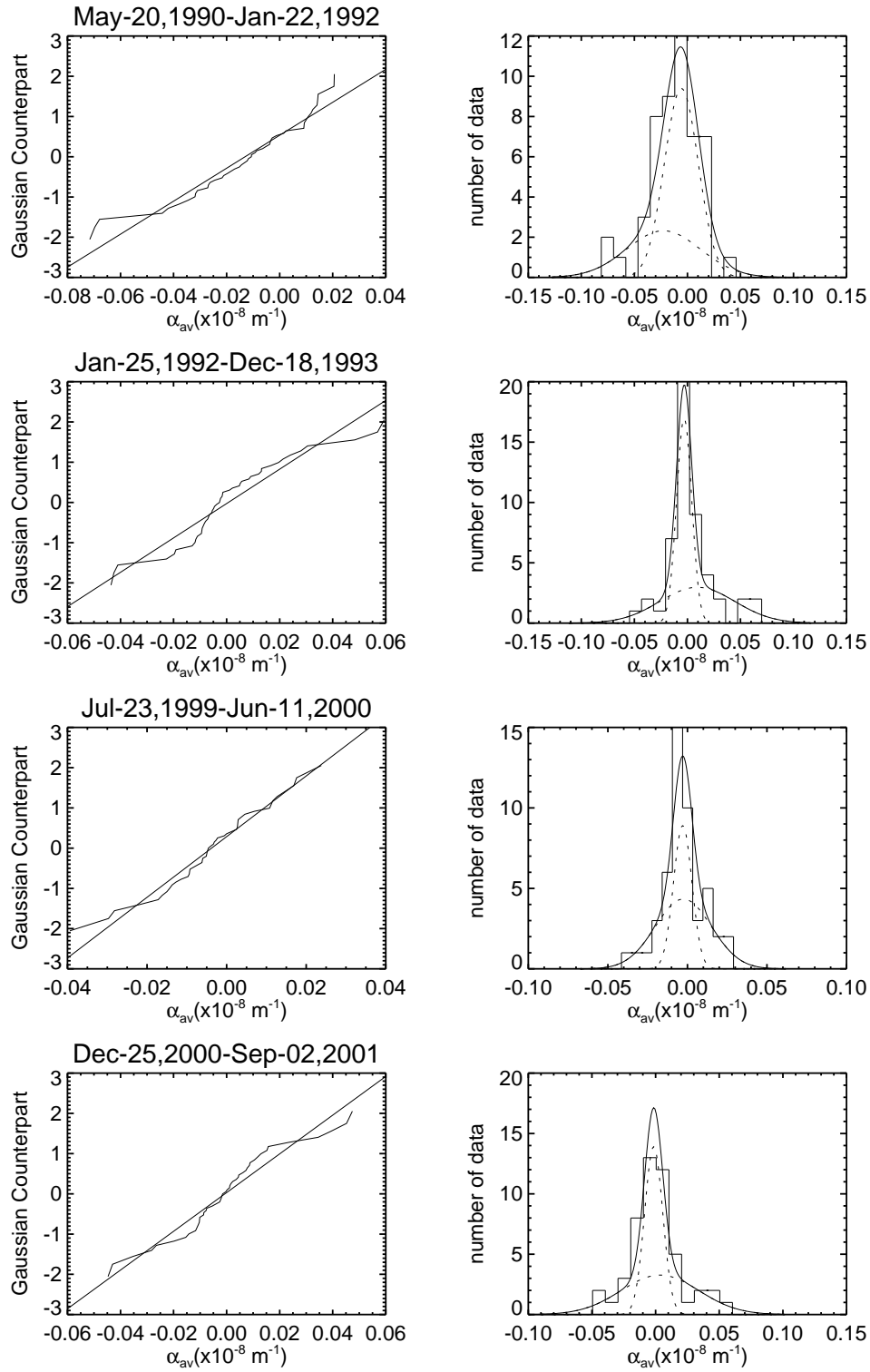


Figure 2. Four cases of the distributions of α_{av} in the northern hemisphere. The left panels show NPP and are annotated by the start and ending dates of the group. The right panels show the data histogram and decomposed two Gaussians (dotted curves) and their sum (solid curve).

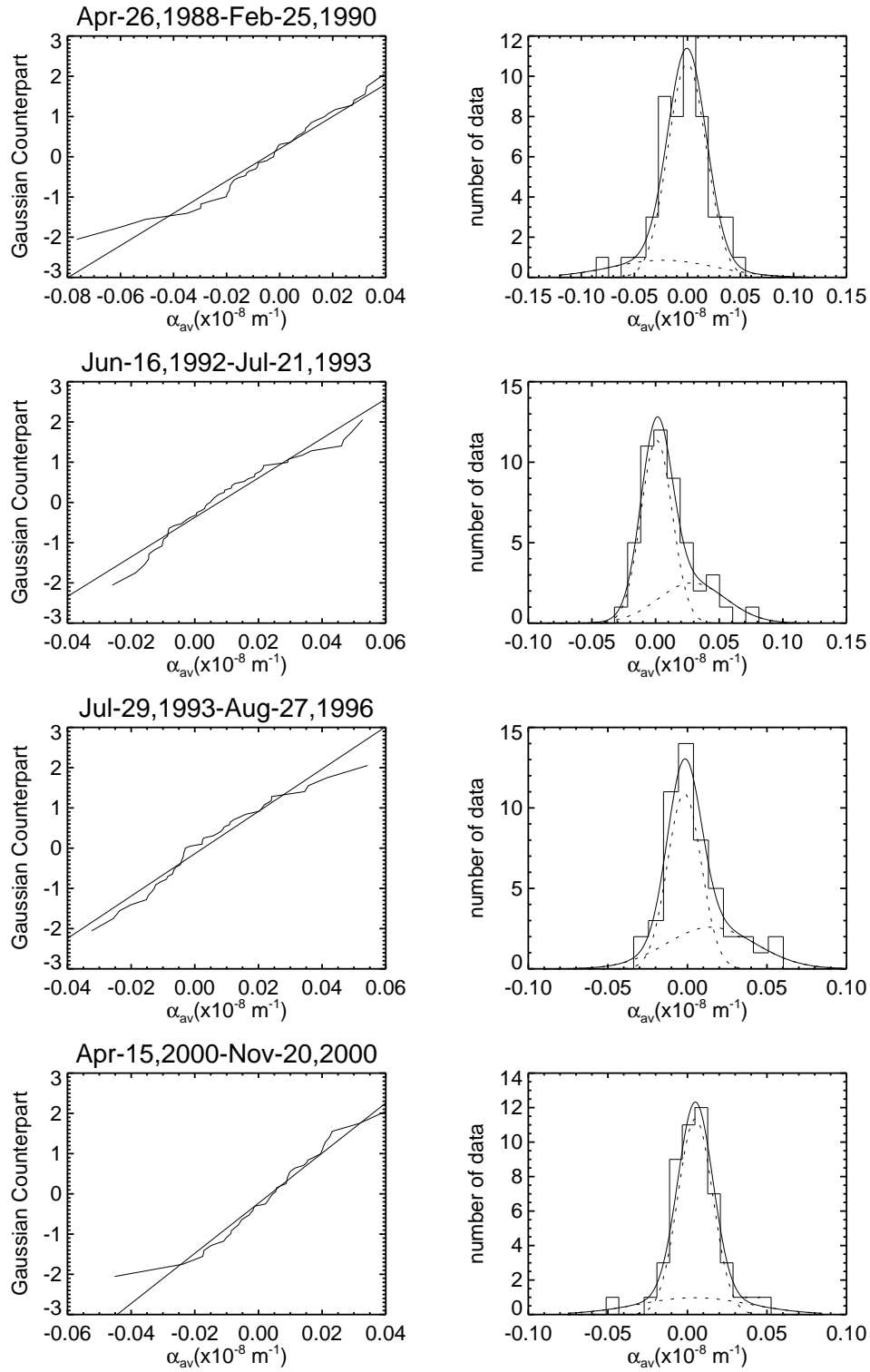


Figure 3. Four cases of the distributions of α_{av} in the southern hemisphere. The left panels NPP and are annotated by the start and ending dates of the group. The right panels show the data histogram and decomposed two Gaussians (dotted curves) and their sum (solid curve).

Table 3. Results of fitting to the data of H_c for ten subgroups in the northern hemisphere.

#	Start	End	δT	μ_0	σ_0	μ_1	σ_1	A_1	μ_2	σ_2	A_2	Error	No
1	Apr-16,1988	May-11,1990	755	-0.0421	0.0758	-0.0268	0.0741	0.8927	-0.1492	0.0198	0.1073	0.0860	50
2	May-20,1990	Jan-22,1992	612	-0.0774	0.2541	-0.0347	0.0953	0.8894	-0.8641	0.5144	0.1106	0.0688	50
3	Jan-25,1992	Dec-18,1993	693	0.0544	0.2714	0.0157	0.1149	0.9140	0.5670	0.9986	0.0860	0.1649	50
4	Dec-26,1993	May-24,1998	1610	-0.0319	0.0814	-0.0268	0.1084	<u>0.6583</u>	-0.0355	0.0132	<u>0.3417</u>	0.2020	50
5	May-31,1998	Jul-22,1999	417	-0.0187	0.0860	-0.0094	0.0668	0.9321	-0.3537	0.1570	0.0679	0.0822	50
6	Jul-23,1999	Jun-11,2000	324	-0.0078	0.0651	-0.0050	0.0748	0.8629	-0.0139	0.0223	0.1371	0.1012	50
7	Jun-12,2000	Dec-21,2000	192	-0.0267	0.0753	-0.0064	0.0476	0.7282	-0.0816	0.1299	0.2718	0.1168	50
8	Dec-25,2000	Sep-02,2001	251	-0.0154	0.0677	-0.0043	0.0480	0.9682	-0.3474	0.0013	0.0318	0.1337	50
9	Sep-22,2001	Jun-28,2003	644	-0.0228	0.1047	-0.0075	0.1297	0.7312	-0.0536	0.0287	0.2688	0.0991	50
10	Jul-5,2003	Dec-23,2005	902	-0.0817	0.1614	-0.0030	0.0675	0.7956	-0.4294	0.1380	0.2044	0.0679	14

Table 4. Results of fitting to the data of H_c for eleven data subgroups in the southern hemisphere.

#	Start	End	δT	μ_0	σ_0	μ_1	σ_1	A_1	μ_2	σ_2	A_2	Error	No
1	Apr-26,1988	Feb-25,1990	670	-0.0273	0.1756	-0.0004	0.1008	0.9426	-0.8515	0.1035	0.0574	0.1190	50
2	Mar-08,1990	Aug-11,1991	521	0.0061	0.2285	0.0622	0.0956	0.8886	-0.7620	0.3935	0.1114	0.1403	50
3	Aug-12,1991	May-08,1992	270	0.0492	0.1122	0.0514	0.1234	0.9488	0.0628	0.0078	0.0512	0.0931	50
4	Jun-16,1992	Jul-21,1993	400	0.1195	0.2721	0.0810	0.1102	0.9185	0.6108	1.0473	0.0815	0.2526	50
5	Jul-29,1993	Aug-27,1996	1125	0.0176	0.0735	0.0115	0.0409	0.6867	0.0369	0.1377	0.3133	0.1160	50
6	Nov-29,1996	Apr-23,1999	875	0.0331	0.0810	0.0130	0.0644	0.8737	0.1903	0.0312	0.1263	0.0989	50
7	May-19,1999	Apr-12,2000	329	0.0053	0.0708	-0.0045	0.0386	0.6750	0.0317	0.1284	0.3250	0.0963	50
8	Apr-15,2000	Nov-20,2000	219	0.0385	0.1084	0.0313	0.0547	0.6922	0.0617	0.2106	0.3078	0.1359	50
9	Nov-27,2000	Oct-11,2001	318	0.0254	0.0807	0.0141	0.0438	0.8746	0.1172	0.2507	0.1254	0.1711	50
10	Oct-22,2001	Oct-27,2003	735	0.0198	0.1427	0.0213	0.0527	<u>0.5970</u>	0.0260	0.2490	<u>0.4030</u>	0.1354	50
11	Oct-28,2003	Dec-16,2005	780	-0.0133	0.1155	-0.0173	0.0949	0.8855	-0.4921	0.4071	0.1145	0.0873	19

hemisphere. It is found that four μ_1 's and three μ_2 's violate the HSR. Among them, two cases have both μ_1 and μ_2 violate the HSR. They occur in the epochs ‘‘Apr-26, 1988’’ to ‘‘Feb-25, 1990’’, and ‘‘May-19, 1999’’ to ‘‘Apr-12, 2000’’, respectively. The amplitudes of A_1 are 0.82 and 0.96 and A_2 are 0.18 and 0.04, respectively. Other two A_2 that violate HSR have amplitudes of 0.04 and 0.02, respectively. Some examples are given in Figure 3. The first row shows apparent violation of two components from the HSR. Other three cases show two components clearly, too. However, all of these components obey the HSR.

We also perform comparative analysis for H_c in a similar way. Table 3 shows the fitting results in the northern hemisphere. For example, in Row 3, i.e., from Jan-25, 1992 to Dec-18, 1993, the means of both components μ_1 and μ_2 show violation of the HSR. Their amplitudes are 0.91 and 0.09. This is also consistent with the results obtained for α_{av} . Some examples are given in Figure 4.

Table 4 shows the results of Gaussian fitting/decomposition for H_c in the southern hemisphere. There are three μ_1 's that violate the HSR in Rows 1, 7 and 11, respectively. Their amplitudes are 0.94, 0.68 and 0.89, respectively. In Rows 1 and 11, the second components also violate the HSR, though with smaller component amplitudes of 0.06 and 0.11. Another

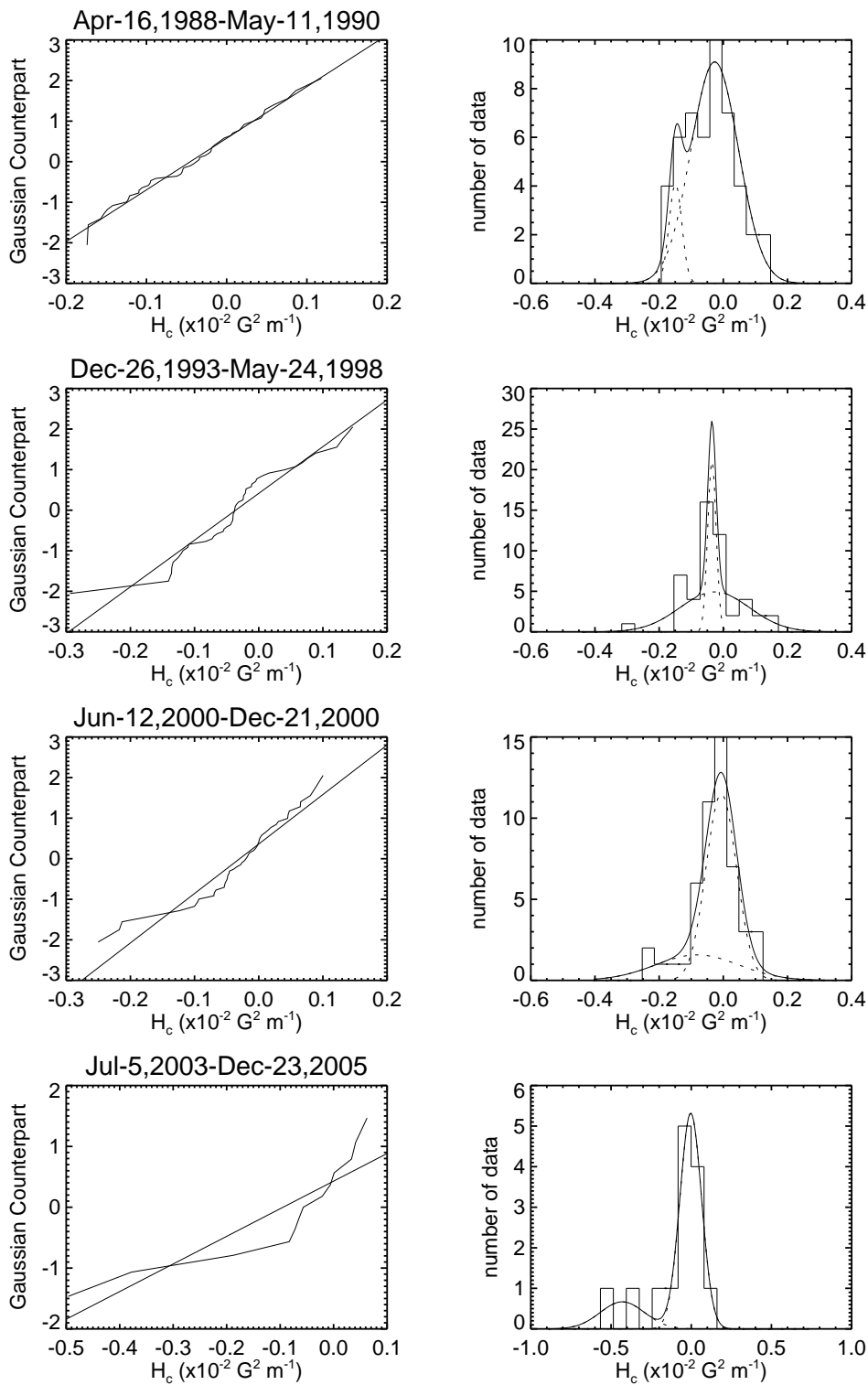


Figure 4. Four cases of the distributions of H_c in the northern hemisphere. The left panels are NPP and are annotated by the start and ending dates of the group. The right panels show the data histogram and decomposed two Gaussians (dotted curves) and their sum (solid curves).

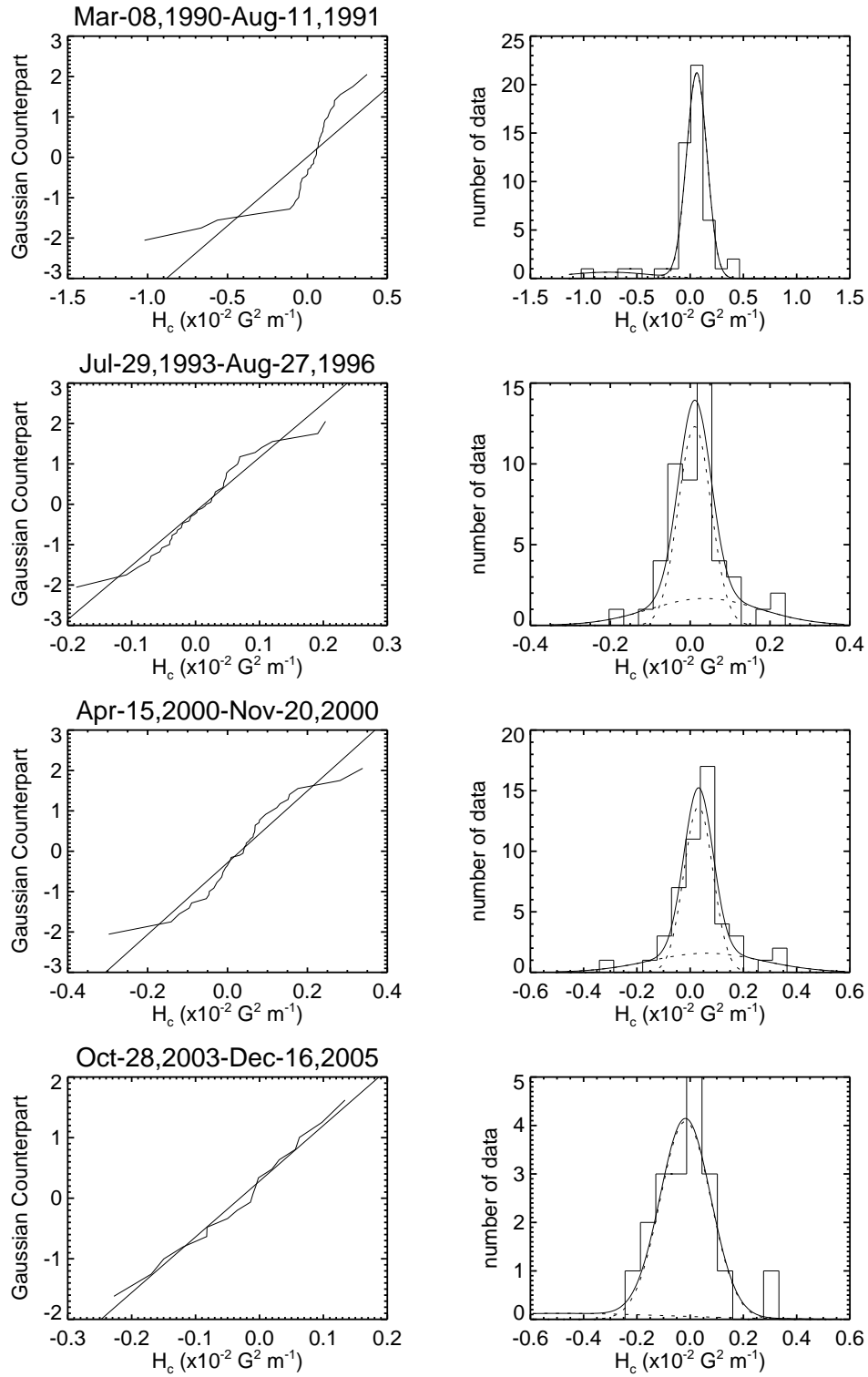


Figure 5. Four cases of the distributions of H_c in the southern hemisphere. The left panels show NPP and are annotated by the start and ending dates of the group. The right panels show the data histogram and decomposed two Gaussians (dotted curves) and their sum (solid curve).

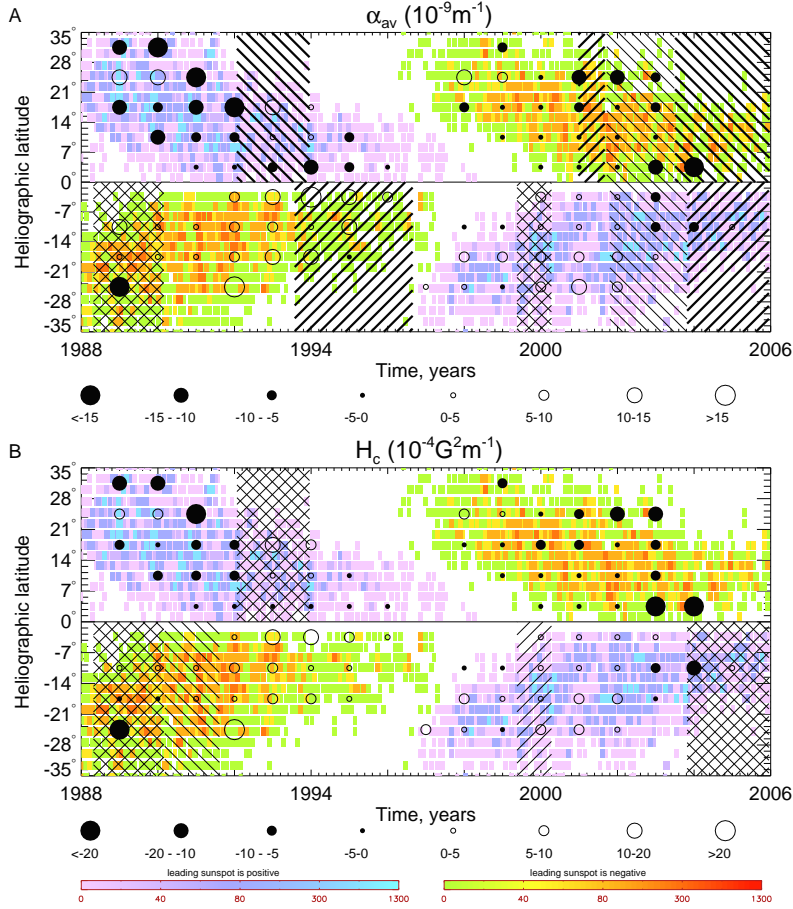


Figure 6. Time-latitude distribution of Gaussian components for selected 983 magnetograms of active regions (one magnetogram per active region) over the period of 1988-2005. The background is the butterfly diagram of current helicity plotted in time-latitude bins as circles over the color plot of sunspot number density. Each bin contains data coming from 7° in latitude and two year running average in time. The 45° and -45° lines mark the epoch in which the main component and sub-component violate the HSR, respectively. The thick lines denote cases when the second component is significant, i.e. the amplitudes satisfy the relation $A_1 < 2A_2$. The upper and lower panels show the results for α_{av} and H_c , respectively.

μ_2 violating the HSR occurs in the epoch of “Mar-08, 1990” to “Aug-11, 1991” (in Row 2); its amplitude is 0.11. Some examples are given in Figure 5.

To compare the epochs where the HSR is violated in the present statistical analysis with the evolution and distribution of α_{av} and H_c obtained in our earlier papers (Zhang et al. 2010), we mark these epochs with the inclined lines of 45° (the first component violates the HSR) and -45° (the second component violates the HSR); see Figure 6. Therefore, the crossed lines represent the cases when both the first and the second components violate the HSR.

Here we estimate the uncertainty in determination of the two Gaussian mean values of the bi-modal distribution of the two parameters α_{av} and H_c under discussion. For that we use the 95 per cent Student’s confidence intervals taking the standard deviations for each Gaussian component σ_i , where $i = 1, 2$, and computing the number of degrees of freedom as

Table 5. Statistical significance of HSR violation for α in the north hemisphere. Numbers in bold indicate violation of HSR, and they are underlined if regarded statistically significant.

#	Start	End	μ_1	$\frac{\sigma_1 t_{n-5}}{\sqrt{n-5}}$	μ_2	$\frac{\sigma_2 t_{n-5}}{\sqrt{n-5}}$
3	Jan-25,1992	Dec-18,1993	-0.0031	0.0018	<u>0.0094</u>	0.0088
8	Dec-25,2000	Sep-02,2001	0.0035	0.0077	-0.0015	0.0018
9	Sep-22,2001	Jun-28,2003	-0.0045	0.0042	<u>0.2665</u>	0.0769
10	Jul-5,2003	Dec-23,2005	-0.0057	0.0129	0.0008	0.0021

Table 6. Statistical significance of HSR violation for α in the south hemisphere. Numbers in bold indicate violation of HSR, and they are underlined if regarded statistically significant.

#	Start	End	μ_1	$\frac{\sigma_1 t_{n-5}}{\sqrt{n-5}}$	μ_2	$\frac{\sigma_2 t_{n-5}}{\sqrt{n-5}}$
1	Apr-26,1988	Feb-25,1990	-0.0003	0.0045	<u>-0.0227</u>	0.0122
5	Jul-29,1993	Aug-27,1996	-0.0019	0.0026	0.0147	0.0070
7	May-19,1999	Apr-12,2000	-0.0001	0.0023	<u>-0.0587</u>	0.0014
10	Oct-22,2001	Oct-27,2003	0.0017	0.0041	<u>-0.0694</u>	0.0010
11	Oct-28,2003	Dec-16,2005	-0.0070	0.0136	0.0010	0.0042

the overall number of available data points in each interval n minus the number of fitting parameters, namely five. Then the expected errors in the mean values of the components would be $\mu_i \pm \sigma_i t_{n-5} / \sqrt{n-5}$, where t_{n-5} is Student's quantile for 95 per cent probability. We consider the violation of the rule significant if the error bars on the mean values that violate the HSR do not contain the zero value of the quantity under consideration. The results are shown in Table 5-8. The mean values which violate the HSR are shown bold, and the cases of significant violation are underlined. The cases for which violation of the HSR is statistically significant are shown in Fig. 7.

The notable features common to two parameters α_{av} and H_c are as follows.

(i) In the 22nd solar cycle there is an epoch of Apr-26, 1988 - Feb-25, 1990 in the southern hemisphere, in which either the first or the second component of both parameters violated the HSR. There is another epoch of Jan-25, 1992 – Dec-18, 1993 in the northern hemisphere, in which the second component of both parameters violated the HSR.

(ii) In the southern hemisphere of the 23rd solar cycle, the first component violated the HSR in the epochs of May-19, 1999 – Apr-12, 2000 and Oct-28, 2003 to Dec-16, 2005.

(iii) Looking at the cases of significant violation of the HSR in terms of Student's error

Table 7. Statistical significance of HSR violation for H_c in the north hemisphere. Numbers in bold indicate violation of HSR, and they are underlined if regarded statistically significant.

#	Start	End	μ_1	$\frac{\sigma_1 t_{n-5}}{\sqrt{n-5}}$	μ_2	$\frac{\sigma_2 t_{n-5}}{\sqrt{n-5}}$
3	Jan-25,1992	Dec-18,1993	0.0157	0.0288	<u>0.5670</u>	0.2500

Table 8. Statistical significance of HSR violation for H_c in the south hemisphere. Numbers in bold indicate violation of HSR, and they are underlined if regarded statistically significant.

#	Start	End	μ_1	$\frac{\sigma_1 t_{n-5}}{\sqrt{n-5}}$	μ_2	$\frac{\sigma_2 t_{n-5}}{\sqrt{n-5}}$
1	Apr-26,1988	Feb-25,1990	-0.0004	0.0252	<u>-0.8515</u>	0.0259
7	May-19,1999	Apr-12,2000	-0.0045	0.0097	0.0317	0.0322
11	Oct-28,2003	Dec-16,2005	-0.0173	0.0544	<u>-0.4921</u>	0.2334

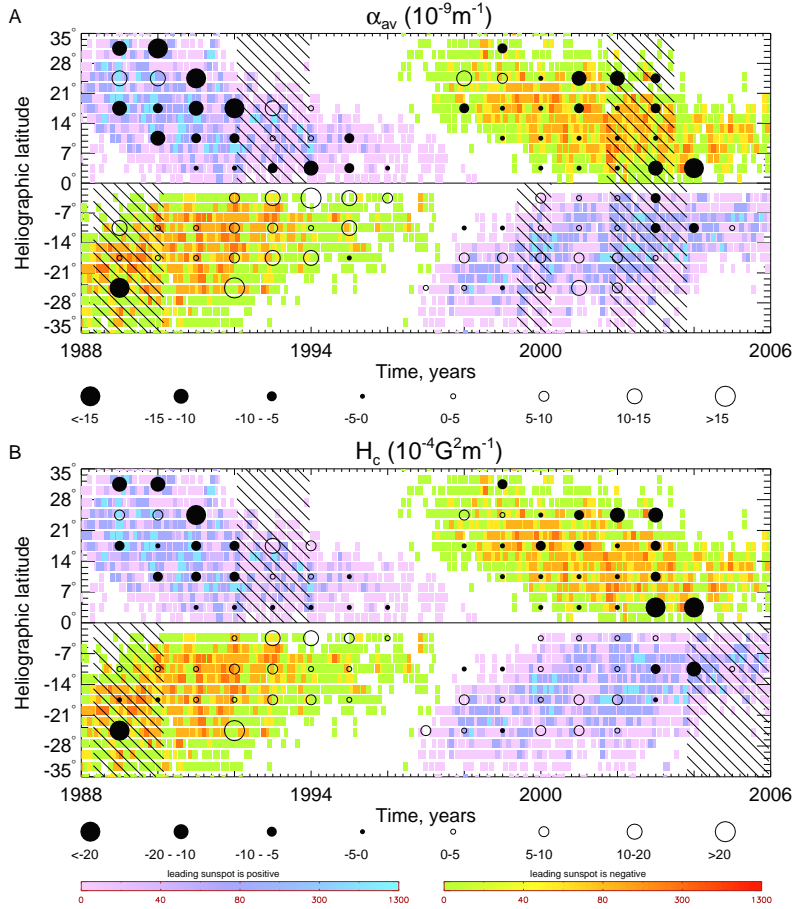


Figure 7. Butterfly diagram with only those cases marked for which violation of the HSR is statistically significant. Notations are the same as in Fig. 6.

bars we note that there are very few of them compared with the the overall cases of violation of the HSR by one or two Gaussian components of the bi-modal distribution.

(iv) We may also note that the cases of significant violation of the HSR occur not in the maximum of the solar cycle but in the phases of rise and fall.

The two parameters α_{av} and H_c showed disparate results as follows.

(i) For α_{av} in the epochs of Dec-25, 2000 – Sep-02, 2001 in the northern hemisphere and Jul-29, 1993 – Aug-27, 1996 in the southern hemisphere, the first component violates the HSR. Also, in the epochs of Sep-22, 2001 – Dec-23, 2005 in the northern hemisphere, the second component violates the HSR. These patches are not found for H_c .

(ii) In the southern hemisphere, the first component of α_{av} violates the HSR in the epoch of Jul-29, 1993 – Aug-27, 1996, the second component of α_{av} violates the HSR in the epochs of May-19, 1999 – Apr-12, 2000 and Oct-22, 2001 – Oct-27, 2003, but these are not seen for H_c . In contrast, the second component of α_{av} does not violate the HSR in the epochs of Mar-08, 1990 – Aug-11, 1991 and Oct-28, 2003 – Dec-16, 2005 but the second component of H_c does violate the HSR during those period.

(iii) The cases of significant violation of the HSR for both parameters α_{av} and H_c coincide for cycle 22 but not for cycle 23. In cycle 23 there is only one case of significant violation of HSR for H_c but three cases for α_{av} . See Fig. 7 for details.

5 DISCUSSION

We have investigated to what extent the current helicity and twist data for solar active regions follow the Gaussian statistics and what kind of message comes from the deviations from the Gaussian distribution.

In our studies we have adopted the method of Normal Probability Paper which has been developed for Gaussian distributions. Of course, there was no reason to believe that the data must be ideally distributed as a Gaussian. However, such analysis has shown relative contributions of the sources of fluctuations as well as the turbulent nature of the measured quantities.

Quite naturally, the statistics of current helicity and twist are not exactly Gaussian. Here we confirmed the previous results of Sokoloff et al. (2008). On the other hand, deviations from Gaussian statistics are rather moderate and it looks often reasonable to discuss the observed statistical distribution for given space-latitude bins as a superposition of two Gaussian distributions with specific means, standard deviations and amplitudes. We have not encountered cases for which such fitting is impossible or insufficient (but see the underlined values of A_2 in Tables 1–4). In other words, we have not detected traces of significant intermittency in solar magnetic fields as its imprints in statistics for the current helicity or twist. We appreciate that the contemporary dynamo theory (see a review by Brandenburg, Sokoloff, and Subramanian 2012) or analysis of the surface solar magnetic tracers (Stenflo 2012) imply that a strong intermittency is expected. Presumably, diffusive processes working during the rise of magnetic flux tubes from the solar interior up to the surface might have strongly smoothed the non-Gaussian features of the distributions.

Formally speaking, the Gaussian distribution of the current helicity was implicitly assumed when one estimates the error bars on the current helicity averaged over a time-latitude bin (e.g., Zhang et al. 2010). In practical respect, however, deviations from Gaussian distribution obtained are small. Due to the Central Limit Theorem in probability theory, one may expect only minor modifications to these estimates and the non-Gaussian nature of distribution can be ignored for this point.

We have isolated several epochs within the time interval covered by observations where deviations from Gaussian statistics look interesting and meaningful. We isolate the time bins with substantial deviations from Gaussian distribution in two ways: when the main Gaussian or the sub-component violates the HSR (Fig. 6), or when the subcomponent is comparable with the main one.

Concerning the violation of the HSR (Fig. 6), we note a substantial north-south asymmetry in the results: main part of the bins with HSR violation belongs to the southern hemisphere. Remarkably, the helicity data for the northern hemisphere for the 23rd cycle during 1997-2006 (with hemispheric averages) do not provide cases with HSR violation at all.

We can summarize our main findings as follows.

1. We have established that for the most of cases in time-hemisphere domains the distribution of averaged helicity is close to Gaussian.
2. At the same time, at some domains (some years and hemispheres) we can clearly observe significant departure of the distribution from a single Gaussian, in the form of two- or multi-component distributions. We are inclined to identify this fact as a real physical property.
3. For the most non-single-Gaussian parts of the dataset we have established co-existence of two or more components, one of which (often predominant) has a mean value very close to zero, which does not contribute much to HSR. The other component has relatively large value, whose sign is sometimes in agreement (for the data in the maximum and shortly after the maximum of the solar cycle), or disagreement (for example of 1989, just at the end of the rising phase of cycle 22) with the HSR.
4. Studies of the locations of the most non-single-Gaussian parts over the time-latitude butterfly diagram shows that these agreement and disagreement are in accord with the global structure of helicity reported by Zhang et al. (2010, cf. their Fig.2).
5. We can interpret the result of multi-component distribution of helicity in terms of the dynamo model which addresses the origin of helicity in solar active regions. For example,

there may be spatial and time domains where the dynamo mechanism does not work, or works differently.

We may note here that the agreement or disagreement with HSR at some latitudes and times may be understood within the framework of solar dynamo models (see, e.g. Zhang et al. 2012 and references therein). Discussion on the applicability of particular dynamo models is beyond the framework of this paper and will be addressed in our forthcoming studies.

6. Another possible interpretation is that the active regions which belong to multi-component distribution are intrinsically different and formed at different depth or by different mechanism.

7. We may suggest that the formation of current helicity in solar active regions may in general occur due to various physical mechanisms at various scales. However, detailed investigation on these mechanisms are yet to be done. This challenges both the dynamo theory as well as the theory of flux tube/active region formation.

ACKNOWLEDGMENTS

This work is partially supported by the National Natural Science Foundation of China under the grants 11028307, 10921303, 11103037, 11173033, 41174153, 11178005, 11221063, by National Basic Research Program of China under the grant 2011CB811401 and by Chinese Academy of Sciences under grant KJCX2-EW-T07 and XDA04060804-02. D.S. and K.K. would like to acknowledge support from Visiting Professorship Programme of Chinese Academy of Sciences 2009J2-12 and thank NAOC of CAS for hospitality, as well as acknowledge support from the NNSF-RFBR collaborative grant 13-02-91158 and RFBR under grants 12-02-00170 and 13-02-01183.. K.K. would like to appreciate Visiting Professorship programme of National Observatories of Japan. We thank the anonymous referee for his/her comments and suggestions that helped to improve the quality of this paper.

REFERENCES

- Abramenko V. I., Wang T. J., Yurchishin V. B., 1996, *Solar Phys.*, 168, 75.
 Bao, S.D., Zhang, H.Q.: 1998, *ApJ*, 496, L43.
 Bao, S.D., Ai, G.X., Zhang, H.Q.: 2001, in *Recent Insights into the Physics of the Sun and Heliosphere - Highlights from SOHO and Other Space Mission*, eds. P. Brekke, B. Fleck, and J. B. Gurman, *IAU Symp.*, No. 203, 247.

- Brandenburg, A., Sokoloff, D. and Subramanian, K., : 2012, *Space Science Reviews*, 169, 123.
- Chernoff, H. and Lieberman, G.J. Use of Normal Probability Paper, 1954, *J. Am. Stat. Assoc.*, 49, No. 268 (Dec., 1954), 778-785.
- Hagino, M., Sakurai, T., 2004, *PASJ*, 56, 831.
- Hagino, M., Sakurai, T., 2005, *PASJ*, 57, 481.
- Hao, J., Zhang, M., 2012, *ApJ*, 733, L27.
- Kleorin, N., Kuzanyan, K., Moss, D., Rogachevskii, I., Sokoloff, D. & Zhang, H. 2003, *A&A*, 409, 1097.
- Parker, E. 1955, *ApJ*, 122, 293.
- Pevtsov, A. A., Canfield R. C., & Metcalf T. R. 1995, *ApJ*, 440, L109.
- Seehafer, N.: 1990, *SoPh*, 125, 219.
- Sokoloff, D., Zhang, H., Kuzanyan, K.M., Obridko, V.N., Tomin, D.N., Tutubalin, V.N., 2008, *Sol. Phys.*, 248, 17.
- Stenflo, J.O., 2012, *A&A*, 541, 17.
- Zhang, H.Q., Bao, S., and Kuzanyan, K.: 2002, *Astron. Rep.*, 46, 424.
- Zhang, H., Sokoloff, D., Rogachevskii, I., Moss, D., Lamburt, V., Kuzanyan, K. & Kleorin, N. 2006, *MNRAS*, 365, 276.
- Zhang, H.Q., Sakurai, T., Pevtsov, A., Gao, Y., Xu, H.Q., Sokoloff, D.D. and Kuzanyan, K.: 2010, *MNRAS*, 402, L30.
- Zhang, H., Moss, D., Kleorin, N., Kuzanyan, K., Rogachevskii, I., Sokoloff, D., Gao, Y., Xu, H., 2012, *ApJ*, 751, 47.